

# VALIDATION OF *DEFSTRA* WATER FILM DEPTH PREDICTION MODEL

Lorenzo Domenichini – Università degli Studi di Firenze  
Giuseppe Loprencipe – Università degli Studi di Roma “La Sapienza”

## ABSTRACT

Water film thickness is one of the main variables influencing the friction values available in the tyre-pavement contact area. Water film depth is influenced by rainfall intensity, grades and cross slopes, length of draining path and pavement texture.

During the EU funded VERT and VERTEC research projects an empirical model allowing to evaluate water film depth on constant slope surfaces, having different textures, was developed. The model was afterwards theoretically extended to consider variable slope surfaces and was included in the VERT MBS vehicle model for driving simulations on varying road surfaces in dangerous conditions.

The experimental validation of the variable slope water flow model has been implemented by means of a full scale physical road model constructed in the Road Laboratory at the University of Florence. The 3,5 m wide per 24 m long model has a longitudinal grade of 2% and a cross slope varying between +1,5% and – 1,5%. The model is equipped with an artificial rainwater simulation system allowing to simulate rain intensities between 20 and 100 mm/h.

The paper will describe the setting up of the road physical model, its calibration and the experimental program performed to validate the water flow model. The results of the experimental study are presented and discussed.

# VALIDATION OF *DEFSTRA* WATER FILM DEPTH PREDICTION MODEL

## INTRODUCTION

The presence of a water film on the road surface produces a notable reduction of the friction available in the tyre-pavement contact area.

Driving on a wet road surface is always characterized by a greater risk: under some conditions, especially at high speed and with high water film thicknesses, the control of the vehicle can result very difficult due to the fact that the friction available in the tyre-pavement contact area decreases to values lower than to those required to safely handle the driving task. In addition, the splash and spray of water produced by the vehicle running over a flooded surface causes the reduction of the driving visibility and this can impair road safety as well.

It is therefore useful to know, in both the design phase and in service conditions, the relationship existing between the road geometry (planimetric and altimetric layout, cross section etc), the pavement surface characteristics (texture, skid resistance, unevenness), the rainfall intensities and the water film depth existing on the pavement surface.

During the EU funded VERT research project (BRPR – CT97- 0461) an empirical model allowing to evaluate the water film depth on constant slope surfaces, having different textures, was developed (Mancosu, Parry, La Torre, 2000). It was included in the VERT MBS vehicle model for the simulation of driving manoeuvres in dangerous situations. The model was further validated within the VERTEC EU funded research project (GRD2 – 2001 – 50007) and theoretically extended to consider variable slope surfaces.

The present paper refers about the experimental activities performed to validate the model developed.

## WATER FILM DEPTH PREDICTION MODELS FOR ROAD SURFACES

Several types of analytical flow models are available in literature for predicting the water depth on the pavement surface in steady-state flow conditions. They can be classified according to the following categories:

- one-dimensional models;
- two-dimensional models;
- depth of flow over porous pavements.

In these models, the calculated water depth (denoted with  $y$  or  $WD$ ), is the average water depth over the pavement mean texture depth and the water film thickness  $WFT$  is the water thickness above the pavement roughness. As a result, the difference between  $WD$  and  $WFT$ , gives the pavement surface mean texture depth  $MTD$  (Figure 1).

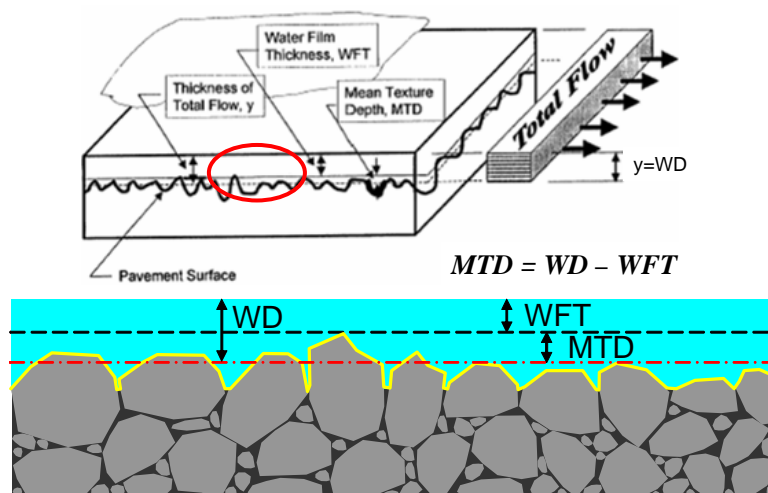


Figure 1 – Definition of water depth  $WD$  (NCHRP, 1998).

An interactive computer program (called *DEFSTRA* – Domenichini & Loprencipe, 1997) was developed by the Authors for predicting the steady state water depth  $WD$  caused by a rainfall of given intensity.

The analytical approach used in DEFSTRA program is a bi-dimensional flow model. It numerically treats the surface geometry data to evaluate the water flow lines over the pavement surface. The area between two consecutive flow lines defines a flow tube or channel. Applying the principle of hydraulic equilibrium of inflow and of outflow delivery  $Q_{IN}=Q_{OUT}$  in steady-state condition (equation (1)) to all the flow tubes over the pavement surface and imposing  $WD=0$  at the initial section of all the flow tubes (belonging always to the crest line of the surface), the water depth value at each point of the surface ( $WD_i$ ) can be evaluated by means of equation (2).

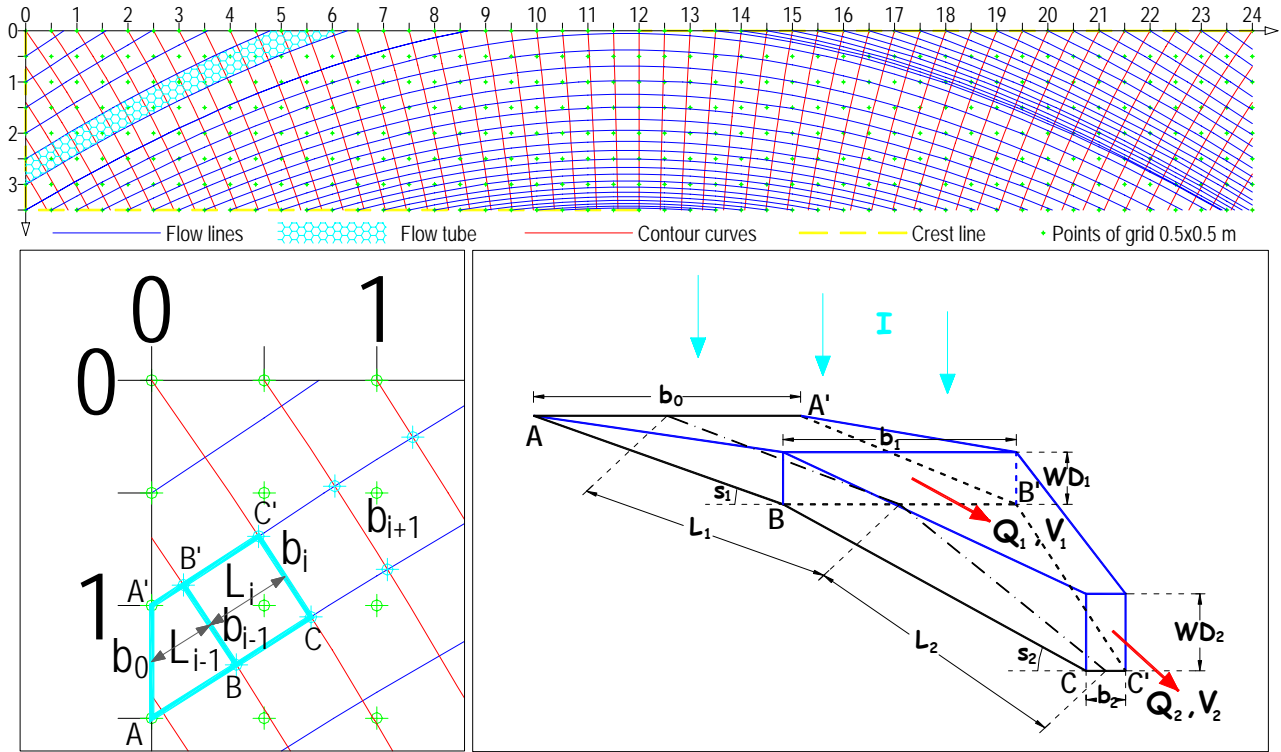


Figure 2 – Analytical formulation used in DEFSTRA computer program for calculating  $WD_i$ .

$$Q_{IN} = \frac{b_i + b_{i-1}}{2} \cdot L_i \cdot I + V_{i-1} \cdot WD_{i-1} \cdot b_{i-1} = Q_{OUT} = V_i \cdot WD_i \cdot b_i \quad (1)$$

$$WD_i = \frac{b_i + b_{i-1}}{2 \cdot b_i} \cdot \frac{L_i \cdot I}{V_i} + \frac{V_{i-1}}{V_i} \cdot WD_{i-1} \cdot b_{i-1} \quad (2)$$

The meaning of the symbols and captions used in equation (1) and equation (2) is clarified in Figure 2. The water flow speed  $V_i$ , variable along each flow tube, may be obtained using any of the proposed experimental formulations of a mono-dimensional flow model on the road pavement available in literature. A unique formulation, given in equation (3), can in fact represent all the experimental research results in terms of water depth:

$$WD = K \cdot \frac{L^m \cdot I^n \cdot MTD^q}{S^r} \quad (3)$$

where:

- $WD$ : water depth [cm];
- $K$ : experimental coefficient [dimension such to give  $WD$  in cm];
- $L$ : drainage path length [m];
- $I$ : rainfall rate [cm/h];
- $MTD$ : mean texture depth [mm];
- $S$ : slope of the drainage path [%].

Besides, in the case of mono-dimensional flow (parallel flow lines), the speed  $V$  can be calculated for an unitary cross section of flow tube and for a drainage path length  $L$ , by means of equation (4).

$$V = \frac{Q}{WD} = \frac{1 \cdot L \cdot I}{WD} \Rightarrow V_i = K \cdot \frac{1}{L_i^n} \cdot L_i^{1-m} \cdot MTD^{-q} \cdot S^{\frac{r}{n}} \cdot WD_i^{\frac{1}{n-1}} \quad (4)$$

Substituting the equation (4) in the equation (2) the general equation (5) can be obtained. It allows to determine, for a given rainfall intensity  $I$ , the water depths  $WD$  along each flow tube knowing the geometric and texture characteristics of the pavement surface.

$$WD_i = \left( \frac{b_i + b_{i-1}}{2 \cdot b_i} \right)^n \cdot L_i^m \cdot I^n \cdot MTD^q \cdot K \cdot S_i^{-r} + \left( \frac{L_{i-1}}{L_i} \right)^{n-m} \cdot WD_{i-1}^n \cdot b_{i-1}^n \quad (5)$$

The evaluation of the coefficient and of the exponents of expression (3) and (5), can be made starting from the experimental data available in literature. The experimental research of Ross and Russam (1968), in which an asphalt concrete pavement with chipping ( $MTD=0.24$  mm) and cement concrete pavement with grooves ( $MTD=0.18$  mm) were used, gave, as a result, equation (6)

$$WD = 0.015 \cdot \frac{(L \cdot I)^{0.5}}{S^{0.2}} \quad (6)$$

in which the coefficient and exponents are:

$$K = 0.015; m = n = 0.5; q = 0; r = 0.2;$$

As can be noted, the variable  $MTD$  is not explicitly shown in equation (6).

From 1971 to 1979, Gallaway et al, processing more than 1000 measurements of water depth on several types of road pavements, obtained equation (7):

$$WD = 0.00693 \cdot \frac{L^{0.519} \cdot I^{0.562} \cdot MTD^{0.125}}{S^{0.364}} \quad (7)$$

In this equation, the values of the coefficient and exponents are:

$$K = 0.00693; m = 0.519; n = 0.562; q = 0.125; r = 0.364;$$

Equation (7) explicitly considers the influence of the variable  $MTD$  on the  $WD$  values.

Recently, during the EU funded VERT project (Università degli Studi di Firenze, 2000), an empirical model allowing to evaluate the water film depth on variable slope surfaces were developed; the index representing the pavement texture used in this research is the MPD (mean profile depth); using the well-known regressive experimental relationship between MPD and ETD (estimated texture depth, which is comparable with  $MTD$ ), an equation similar to (3) can be obtained:

$$WD = 0.016405 \cdot \frac{L^{0.4} \cdot I^{0.4} \cdot MTD^{0.4}}{S^{0.3}} \quad (8)$$

In this latter case, the coefficient  $K$  and the exponents  $m$ ,  $n$ ,  $q$  and  $r$  are the following:

$$K = 0.016405; m = 0.4; n = 0.4; q = 0.4; r = 0.3;$$

For a pavement surface having a  $MTD$  value of 0.18 mm with a maximum drainage path length  $L$  equal to 10 m, a slope of the drainage path  $S$  equal to 2.5 % and a rainfall intensity  $I$  equal to 5 cm/h, the  $WD$  values calculated by means of the three aforesaid formulations are shown in the Figure 3.

A sensitivity analysis of the three models was performed and shown an interesting result: for slopes of the drainage path similar to that existing in straight sections of road pavement (2.5 %), the  $WD$ s calculated by means of Gallaway's equation are middle respect to those calculated by means of other two formulations; if the slope increases, the Gallaway  $WD$ s are brought near to Ross & Russam  $WD$ s and if decreases, the Gallaway  $WD$ s are brought near to VERT  $WD$ s.

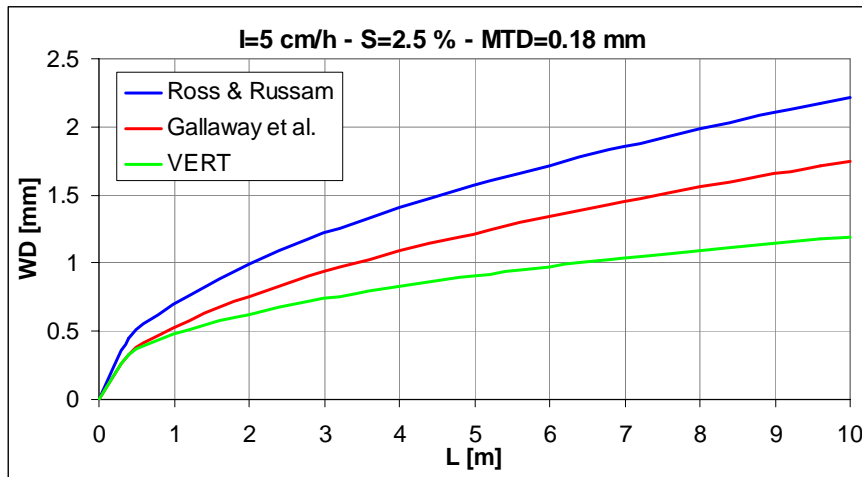


Figure 3 – Comparison between the three flow formulation considered.

In conclusion, the DEFSTRA computer program, by means of equation (5), allows to calculate the WDs along all the water flow tubes of any road surface, allowing the user to choose each one of the three formulations above considered. The algorithm of the program has been afterward slightly modified to account the specific situations encountered during its validation. The modifications included the possibility to account for spatially variable rainfall intensities (the procedure used when the rainfall intensity is variable from cell to cell is shown in Figure 4) and for assigning a WD to each cell, starting from the WDs calculated along the water flow tubes.

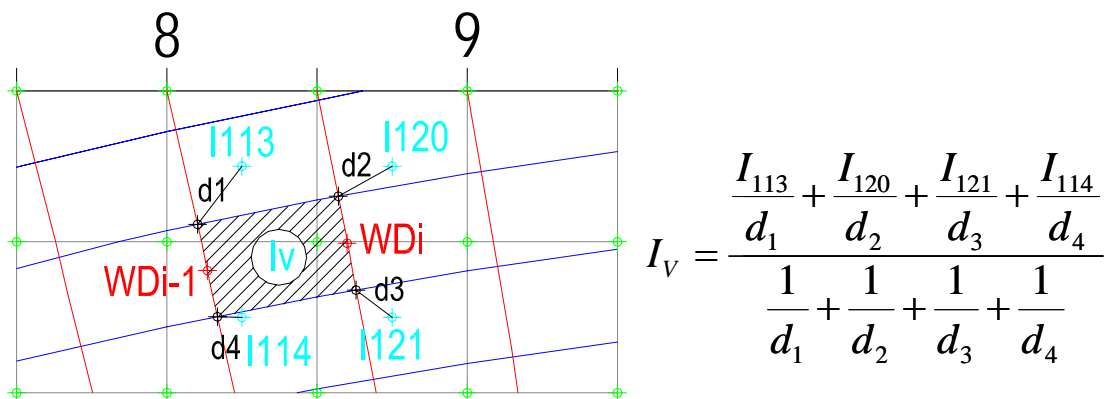


Figure 4 – Procedures of calculus used for the experimental case to take account of variability of rainfall intensity.

## FULL SCALE MODEL FOR THE EXPERIMENTAL VALIDATION OF DEFSTRA COMPUTER PROGRAM

A full scale physical model has been constructed at the road laboratory of the University of Florence to reproduce the flow of the water on a road surface during artificial rain events. The geometry of the model (longitudinal slope and cross slope) reproduces a road transitional zone where the cross slope changes to accommodate an horizontal curve according to the Italian road design standards. The model includes the construction of an artificial rain system allowing rainfalls of adjustable intensity. The model is finally equipped with a water collection system, able to re-circulate the water flowed over and out the road test surface.

### Geometry and Structure of the Road Model

The full scale road surface model has a width of 3.5 m, a length of 24 m of, has a constant longitudinal slope of 2% and a cross slope variable from +1.15% (up) to -1.15% (down); the rotation axle of the platform coincides with the left edge.

The pavement structure consists of a 5 cm thick a concrete slab cast on a corrugated iron sheet (7.5 cm of thickness) filled with expanded clay; it is supported by at steel bearing structure composed by pillars and beams (Figure 5 and Figure 6).

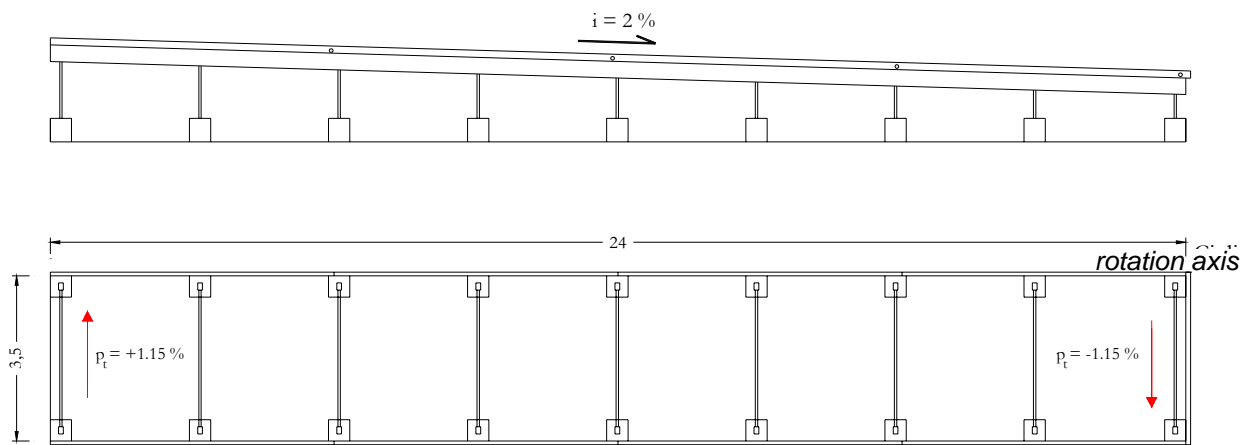


Figure 5 – Plan and lateral prospect of the structure.

The concrete slab surface is finished with a cement mortar lying and a waterproofing membrane. The pavement surface was finally treated with a smooth reference finishing layer (with no texture) and, afterward, with two different surface treatments having different textures.

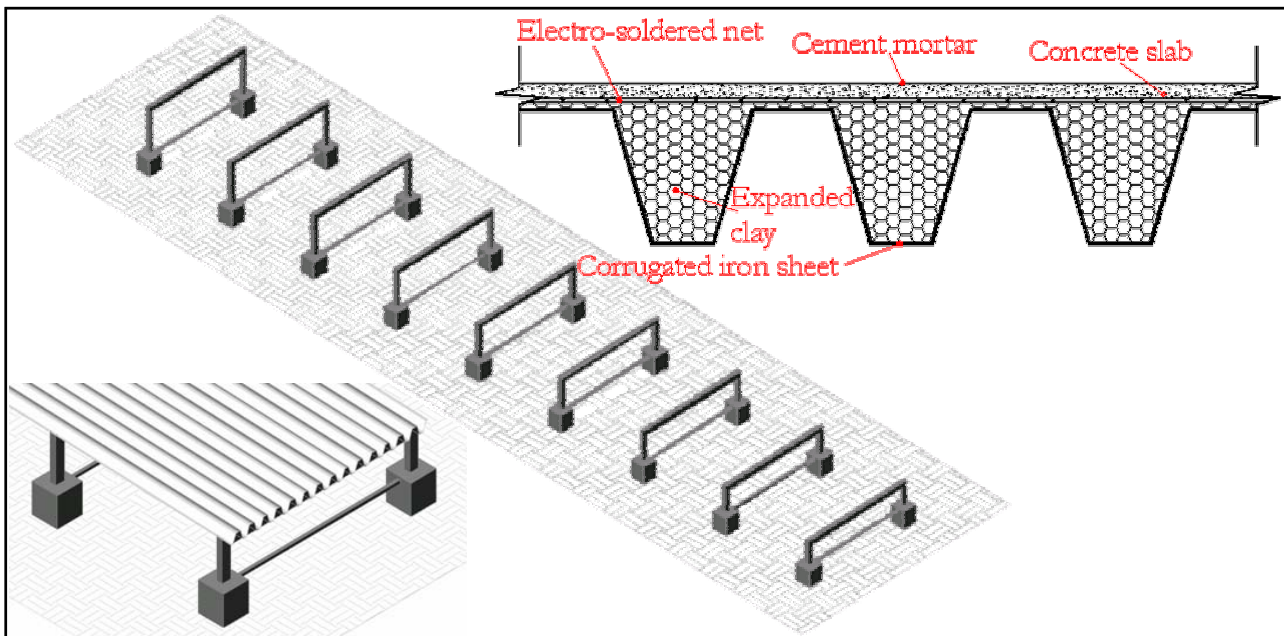


Figure 6 – Axonometric projection of structure and pavement layers.

The model has been built inside a shed (Figure 7), in order to have a closed environment in which it was possible to reproduce the required rainfalls events and, at the same time, to have the possibility to preserve from the atmospheric agents all the equipments used for the tests (pipelines, tanks, pumps, tools for the measurements, etc).

### Artificial rain system

The water plant simulating the rain is a closed system subdivided in four parts:

- **Adduction plant** from the water main.
- **Accumulation plant** with water tanks and circulation pumps.
- **Artificial rainfall plant** with nebulizers and sprinklers.
- **Water recycling plant** to return the water to the tanks.

The adduction plant (Figure 8) is supplied directly from the aqueduct through a pipe (1") that carries the water in four accumulation tanks each of 1 m<sup>3</sup> of capacity. The adduction plant is linked in only one tank; the other three tanks are filled by means of a levelling pipe net with main tank.



Figure 7 – Front view of surface inside to shed with the reference flat surface.

The water accumulated in the tanks is introduced in the pipes net through a centrifugal pump (Figure 8) with maximum power of 4 KW (minimum delivery:  $Q_{\min}=5 \text{ m}^3/\text{h}$  – maximum delivery  $Q_{\max}=24 \text{ m}^3/\text{h}$ ). The pump sucks from all the tanks, by means of a cross connection.

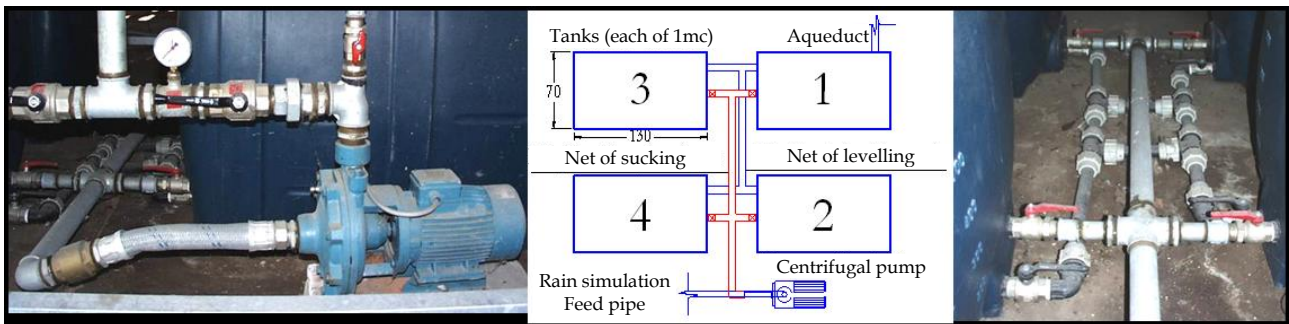


Figure 8 – Centrifugal pump and pipes conduit between the tanks.

A bypass controls the irregular delivery of water and avoids damage to the pump in case the water in the tanks is not enough.

Two valves on the feed pipe allow to regulate the water in the net. A third valve, fitted on the pipe that brings the water in excess to tanks, rules the water flow that is not necessary for the test.

In the feed pipe a filter and a water delivers controller for a best regulation of rainfall rates are fitted.

The artificial rain system consists of a longitudinal pipe placed at 2 m height above the test surface, and 15 transversal pipes placed at 150 cm intervals (Figure 9) and carrying 5 nozzles (Figure 10).

There are two types of nozzles used: the nebulizers “CENTURION” for low rainfall rates and the sprinklers “FULLJET”, for high level of rainfall intensities.

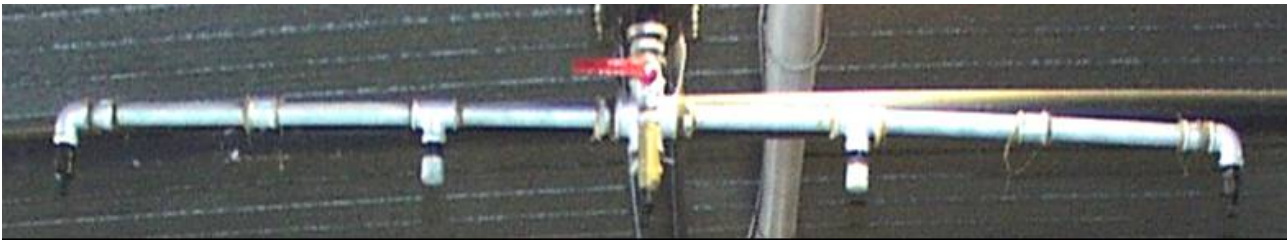


Figure 9 – Transversal line of pipe with nebulizers and sprinklers.



Figure 10 – Transversal lines of pipes and particular of nebulizer CENTURION and sprinkler FULLJET.

For the simulation of the three rainfall intensities used in the experimental program (20-50-100 mm/h) three schemes of nozzles were adopted (Figure 11). The first scheme uses only the nebulizers “CENTURION” placed at the end of transversal pipes; the second scheme uses in addition to the pervious scheme another nebulizer placed in the middle of transversal pipes (with a total of 3 nebulizers for each line). For high rainfall intensity (greater than 50 mm/h) in addition to the pervious scheme, the alternate sprinklers “FULLJET”, placed in the middle of the transversal line are used.

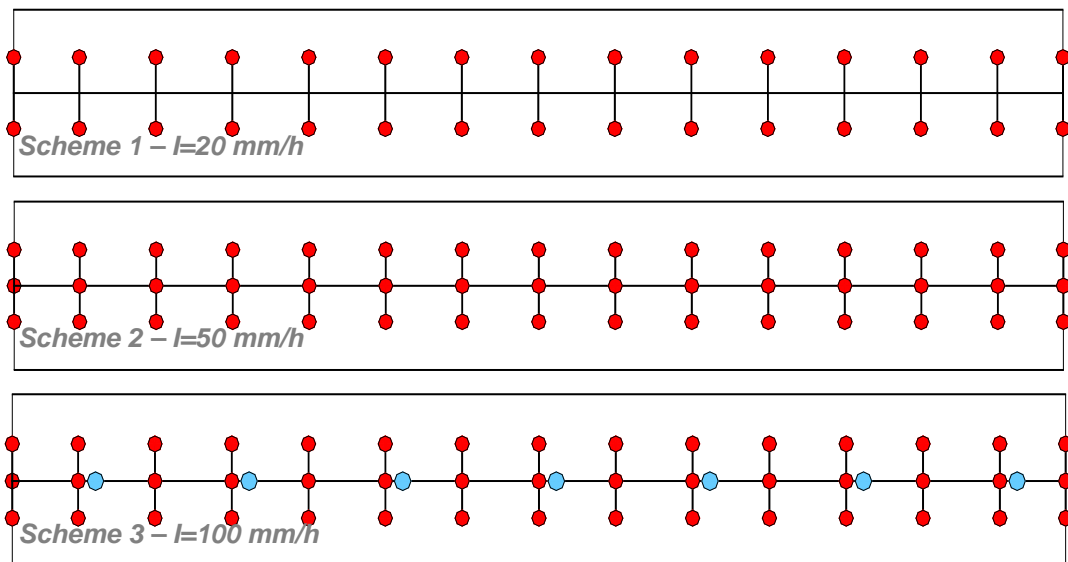


Figure 11 – Schemes of distribution of the nebulizers (in red) and of the sprinklers (in cyan) to simulate 3 rainfall intensities.

The water fallen on the surface flows out inside a perimeter gutter (Figure 12) carrying the water to a system that allows to weigh the water collected (picking up it in a smaller secondary tank with the purpose to know the imposed total value of rain intensity in setting phase), or directly to the accumulation tanks (during the normal use of the model).

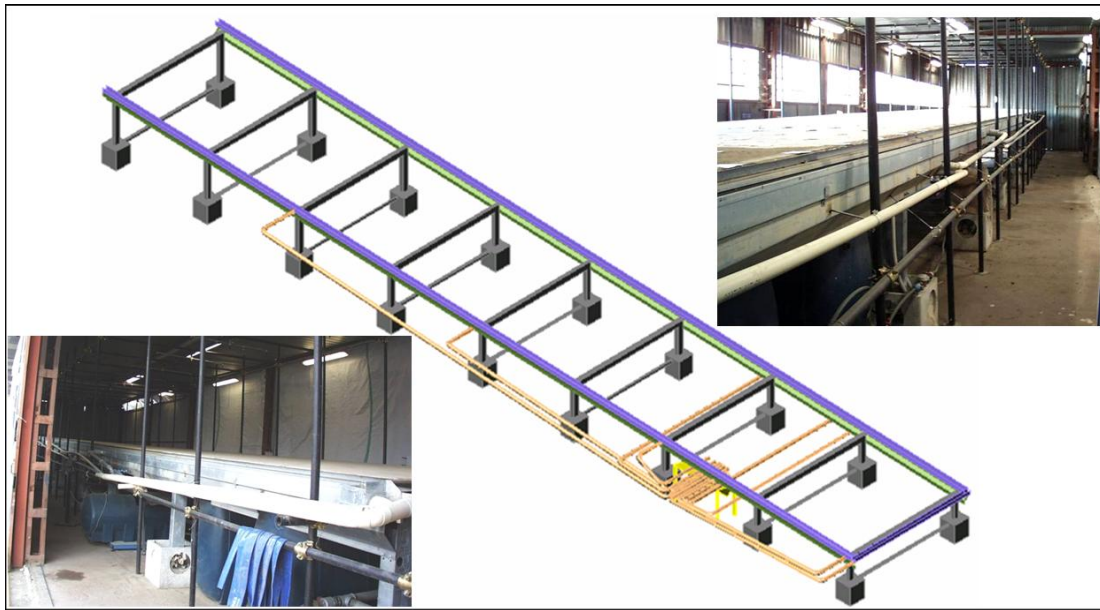


Figure 12 – Hydraulic nets of down pipes.

### Rainfall intensity measurements and setting up the artificial rain system

The rain simulation system is able to reproduce rainfalls with different intensity values. In the experimental program performed three different rainfall intensities were used: 20, 50 and 100 mm/h. The total amount of water fallen on surface was evaluated by means of the above described weighing system; the system measures the mass of out water ( $\Delta M$  is fixed in 100 Kg), in steady-state condition, respect to a time interval  $\Delta t$ . Therefore, the mean rainfall intensity can be obtained with the equation (9) :

$$I_{med} = \frac{\Delta M}{MV_A \cdot S_m \cdot \Delta t} \cdot 3600 \cdot 1000 \quad (9)$$

where:

- $I_{med}$  mean rainfall intensity [mm/h];
- $\Delta M$  increment of reference mass equal to 100 [kg];
- $MV_A$  specific gravity of water equal to 1000 [kg/m<sup>3</sup>];
- $\Delta t$  time necessary to weigh a mass  $\Delta M$  in [s];
- $S_m$  area of model surface equal to 24x3.5=84 [m<sup>2</sup>].

The model setting for having the desired mean rainfall intensity was a very delicate operation.

Even if the maximum attention was played to choose the nozzles choice type and number, their position and distribution on the model, it was not possible to obtain a constant value of rainfall intensity over the entire test surface.

For this reason, a lot of measurements of the actual spatial distribution of the rainfall intensities over the test surface were performed.

To do this, cylindrical containers was positioned in the centre of measurements cell, and, after 10 minutes (600 s) of rain, they were weighted with a precision balance (Figure 13).

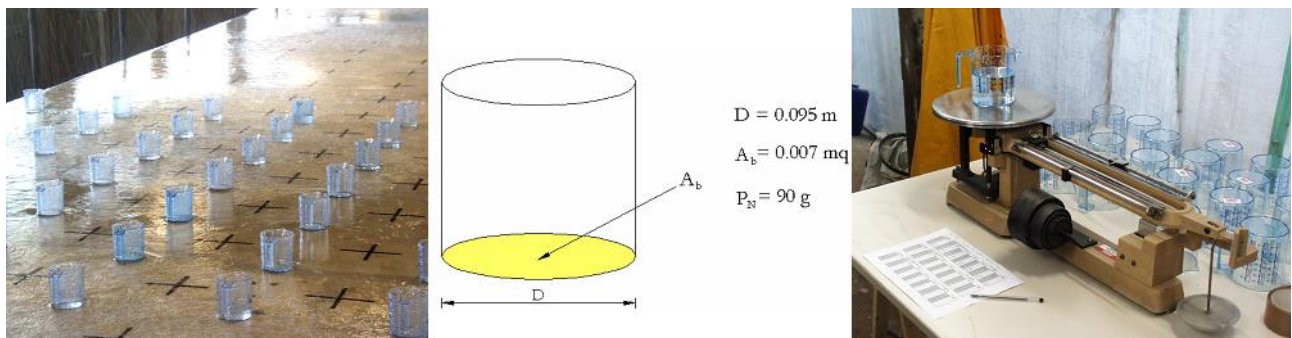


Figure 13 – Positioning of containers on the surface, dimension of containers and their weighting.

The rainfall intensity  $I_j$  for each cell was calculated with the equation (10), known the empty mass  $M_T$  and the base area  $A_B$  of each container:

$$I_j = \frac{(M_{Lj} - M_T)}{MV_A \cdot A_B \cdot T} \cdot 3600 \cdot 1000 \quad (10)$$

where:

- $I_j$ : rainfall intensity in cell  $j$  [mm/h];
- $MV_A$ : specific gravity of water equal to 1000 [kg/m<sup>3</sup>];
- $M_{Lj}$ : water mass collected by container positioned in cell  $j$  [kg];
- $M_T$ : empty mass of container equal to 0.09 [kg];
- $A_B$ : base area of container equal to 0.007 [m<sup>2</sup>];
- $T$ : time of test equal to 600 [s].

The value  $I_j$  measured in the centre of each cell was assigned to the entire area of the cell.

Reproducing, on the base of measurements performed, the rainfall intensity values for all the 336 cells of test surface, the chromatic contour curves diagrams showing the distribution of the actual rain intensities in each portion of the test surface are drawn in Figure 14 for the three rainfall intensities.

The measurements show that, for the three rainfall intensities, the mean of the values  $I_j$  of rain intensities measured on all cells is practically equal to the nominal desired value of rain intensity imposed ( $\pm 0.3\%$ ).

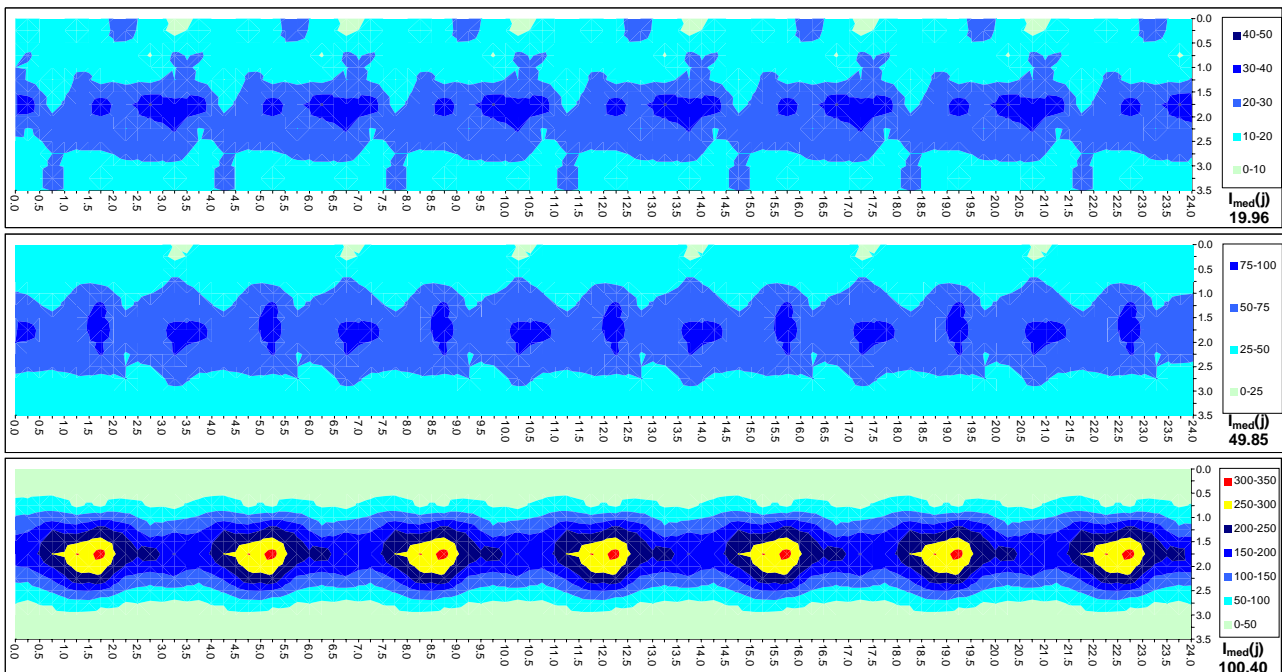


Figure 14 – Variability of the 3 rainfall intensities on test surface.

## Test pavement surfaces

The experimental program to validate the DEFSTRA prediction model provided for the water depth measurement on three types of pavement surface:

- a smooth reference surface, called *surface 0*;
- two surfaces characterized by different textures, called *surface 1* and *surface 2*.

To construct the latter, two different techniques were used:

- 1) *surface 1*: a cold asphalt concrete laid over a tack coat made of bituminous emulsion, and compacted with a heavy portable roller. The layer thickness is resulted about 1 cm (Figure 15);
- 2) *surface 2*: chippings laid on a tack coat made of bituminous emulsion placed over the *surface 1*. The aggregate was compacted and the surplus of chippings removed from surface.

Figure 16 shows the different constructive phases of the surface 2 and Figure 17 shows the chipping grading curve and a view of the finished surface.



Figure 15 – Laying and final view of *surface 1*.



Figure 16 – Laying and final view of *surface 2*.

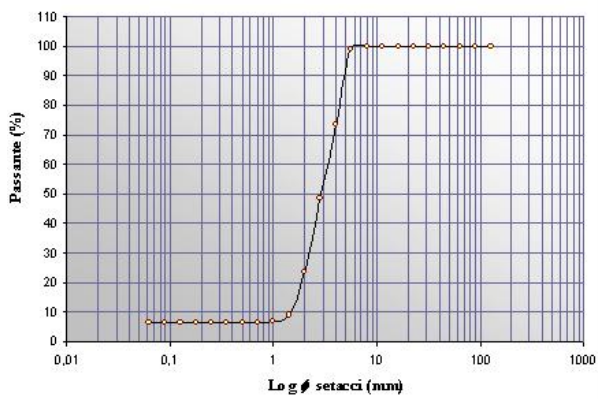


Figure 17 – Grading curve and the view of material of the *surface 2*.

## Characterization tests of the physical model

### Topographic survey of surface

After the building of the structure some deformations of the surface occurred due to consolidation and thermal distortion of the structure. These have been caused the changing of the geometry of the test surface in comparison to the theoretical one.

To quantify the entity of these deformations a precision topographic survey by means of the "close range" photogrammetry technique has been performed on model surface (Figure 18).



Figure 18 – Positioning of camera for one of two clicks of stereocouple.

Such topographic technique consists in the survey of transversal and longitudinal sections of the surface with the definition of one point every 2 cm with millimetric precision.

To reach the required precision, the surface has been divided in four portions with zones of overlapping.

For each zone the method requires a stereocouple that consists in two photos played with camera positioned on tripod (Figure 18); each stereo couple characterizes a digital elevation model (DEM) with width equal to 3.5 m and length variable between 5 m to 7 m.

On the left of Figure 19 the four independent stereocouples are shown. For the determination of the points of support allowing to reassemble the 4 models, another topographical survey has been made with a total station Geotronics shown on the right of Figure 19, supported by a precision leveling to guarantee an accurate definition of the elevations of the surface.

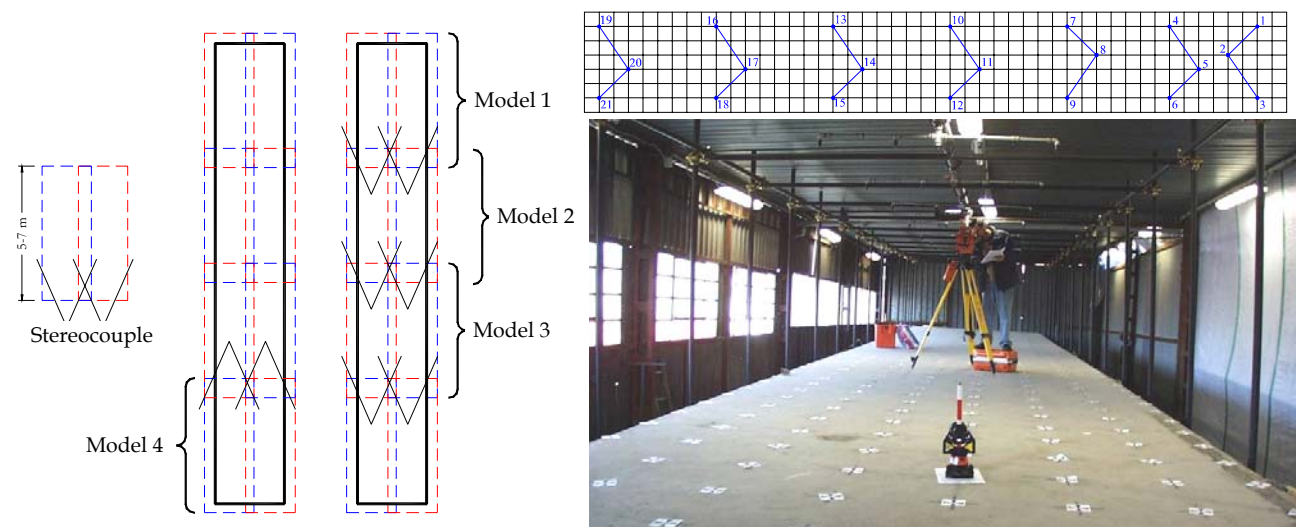


Figure 19 – Stereocouples of the surface and topographic point of support surveyed with total station Geotronics.

The comparison between the theoretical surface and the real surface made with relative contour lines is shown in Figure 20; the grey lines, relative to real surface, show that neither along the edges nor in many portions of the model the differences with the theoretical surface can be neglected.

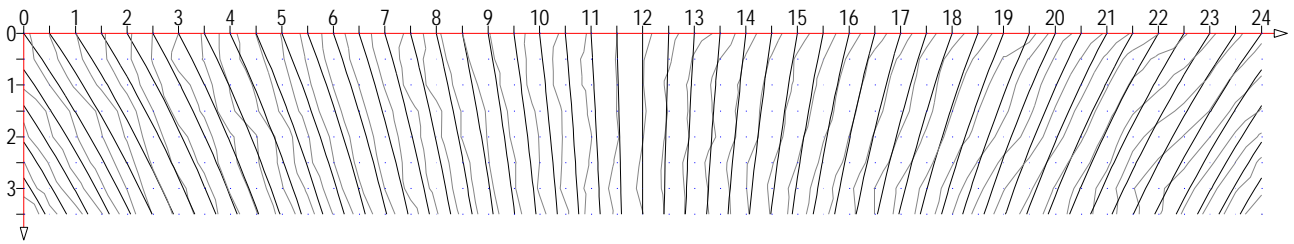


Figure 20 – Contour curves comparing between theoretic surface and real surface.

Such differences could influence the water flow paths on the surface; in Figure 21 the flow lines of the two surfaces are shown; for both the surfaces the flow lines are determined with the computer program DEFSTRA.

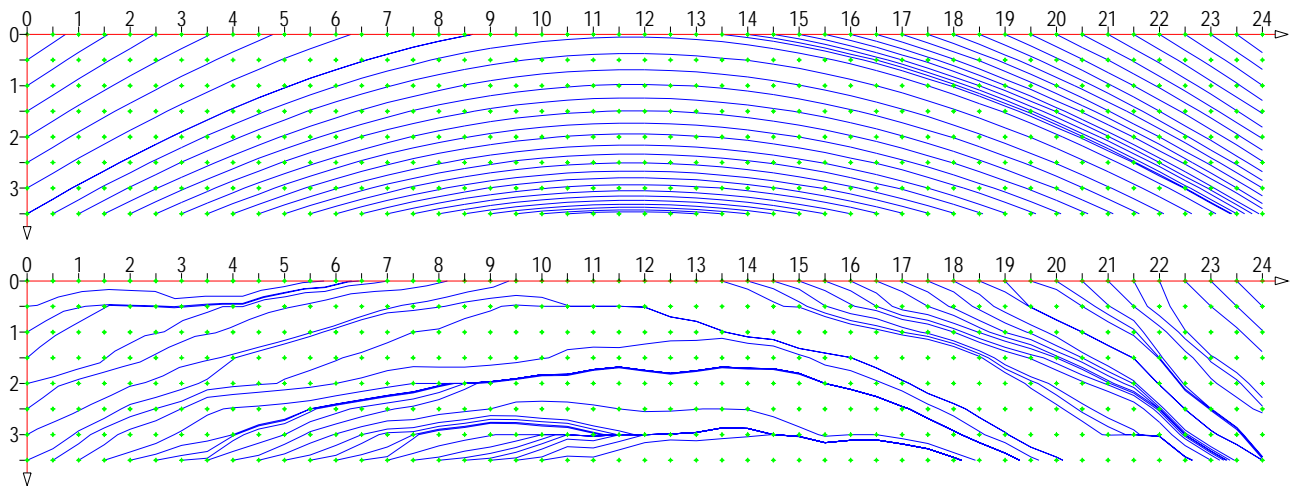


Figure 21 – Flow lines path comparing between theoretic surface and real surface.

To confirm the importance to consider, in the validation process, the real surface instead of the flat theoretical one, a temporal sequence of images during the phase of drying after a simulated rainfall are shown in Figure 22; two preferential paths of water flow are clearly visible.



Figure 22 – Temporal sequence of images during the phase of drying on surface 0.

Tests on functional characteristic of three surfaces

The characteristics of texture of the three test surfaces has been measured with the volumetric method in terms of MTD (Mean Texture Depth). Six measurements (cells n. 37, 39, 41, 296, 298 and 300) for each test surfaces has been made; the Figure 23 shows the positioning of this measurements.

The MTD values obtained for the six cells of the three test surfaces are reported in Table 1; for the two textured pavements, one of the six values is very different to other five; then, in the prevision model DEFSTRA this outsider value has not been considered, calculating the mean value of MTD of these surfaces with five test values.

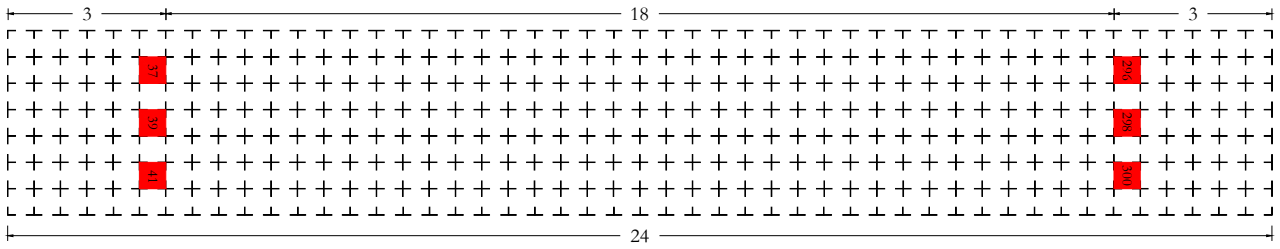


Figure 23 – Positioning of texture measurements.

N. Cell	MTD for the 3 test surfaces (mm)		
	0	1	2
37	0.18	0.88	1.62
39	0.18	0.84	1.51
41	0.18	0.80	1.51
296	0.18	0.98	1.62
298	0.18	0.88	1.51
300	0.18	1.24	1.75
mean	0.18	0.94	1.59
mean no max	<b>0.18</b>	<b>0.88</b>	<b>1.55</b>

Table 1 – Results of texture tests for the three reference surface.

Measurements of water depths

The measurements of the water depths has been made using a device (called limnimeter) developed at the CETE laboratory of Nantes during the VERT project.

The device is able to measure, in real time, the water depths on the surface of the model sending the measurements to a computer wireless linked.

The limnimeter is constituted by two parts both placed on a tripod: the first part is installed in the low side of the support and it measures the water depths; the other part is installed on the top of the tripod and it visualizes the measures (Figure 24).



Figure 24 –Limnimeter in running during the simulated rain.

The part of the device in contact with the water film consists of a iron rod sliding inside a void cylinder. At the down edge of iron rod a truncated cone with two parallel needles is linked; when the bar descends, the needles touch the pavement and the device performs the first reading; after, the rod ascends and the device performs the second reading when the needles touch the upper part of film water. The difference between the two readings gives the water depth.

The truncated cone cover (Figure 25) protects the needles by the water drops to avoid non correct readings. During the measurements, for a best protection of the device, an umbrella is mounted on tripod.

A specific software installed in a notebook (Figure 26) acquires the data and controls the time elapsed between the WD measures. Each measure of WD is the result of 20+20 readings made every 20 seconds.

In the preliminary phase, to evaluate the differences of WD measured inside of generic cell, the device has been placed in five different points of the cell comparing the results (in terms of mean and standard deviation). The results (Figure 27) show that the measure made in the centre of one cell can be considered sufficiently representative of all points of the cell 0.5 m x 0.5 m.

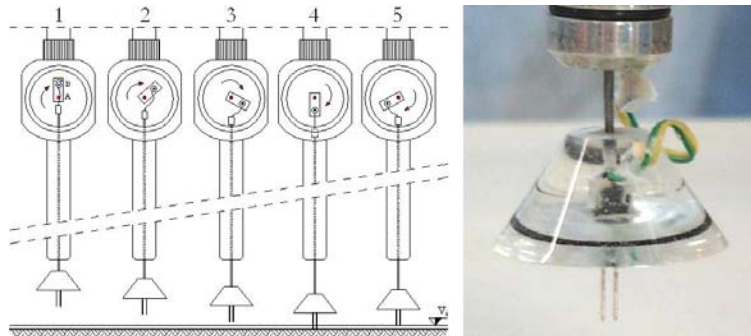


Figure 25 – Running of limnimeter, truncated cone cover and couple of two parallel.

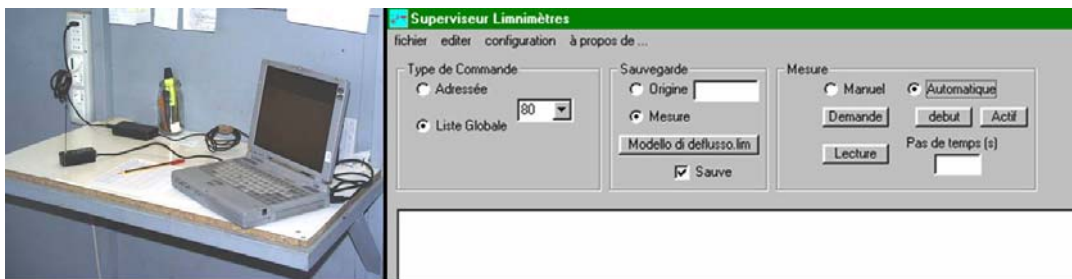


Figure 26 – PC with antenna to download the WD data and software management of device.

Cell position	Mean of 20 readings (mm)	St. Dev. of 20 readings
1	1.09	0.04
2	1.16	0.03
3	1.05	0.03
4	1.04	0.05
5	1.12	0.04
Between the mean	1.09	0.05

Figure 27 – Test and results to evaluate the variability of WD inside of cell.

The measurements of the water depths has been made in the area of the model shown in Figure 28, where the WDs reaches the highest values.

Four alignments (A, B, C and D) for a width of 2.0 m and with length equal to 6.5 m has been chosen (4x13=52 cells) to monitor the WDs for the three rainfall rates and for each surface (total number of WD measurements: 52x3x3=468).

The Figure 29 shows the chromatic contour curves diagrams in terms of WD in the reference area for all cases (the rainfall rates increases from top to down and pavement texture increases from left to right).

The light blue areas represent zones with less WDs (0.5-1.5 mm) while the dark red areas the zones with the highest WDs (> 4.5 mm).

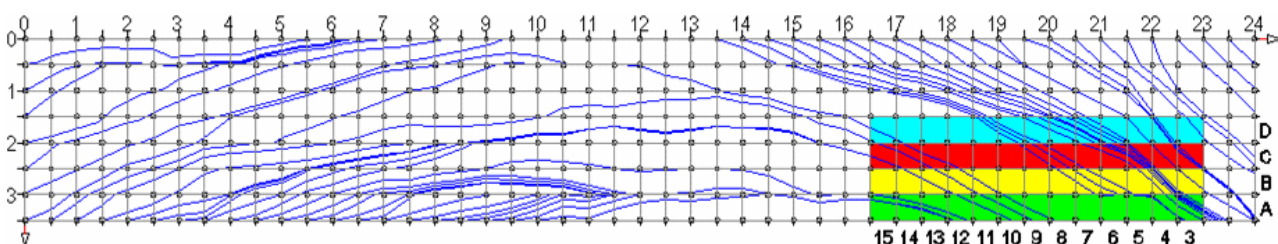


Figure 28 – Reference area for WD measuring.

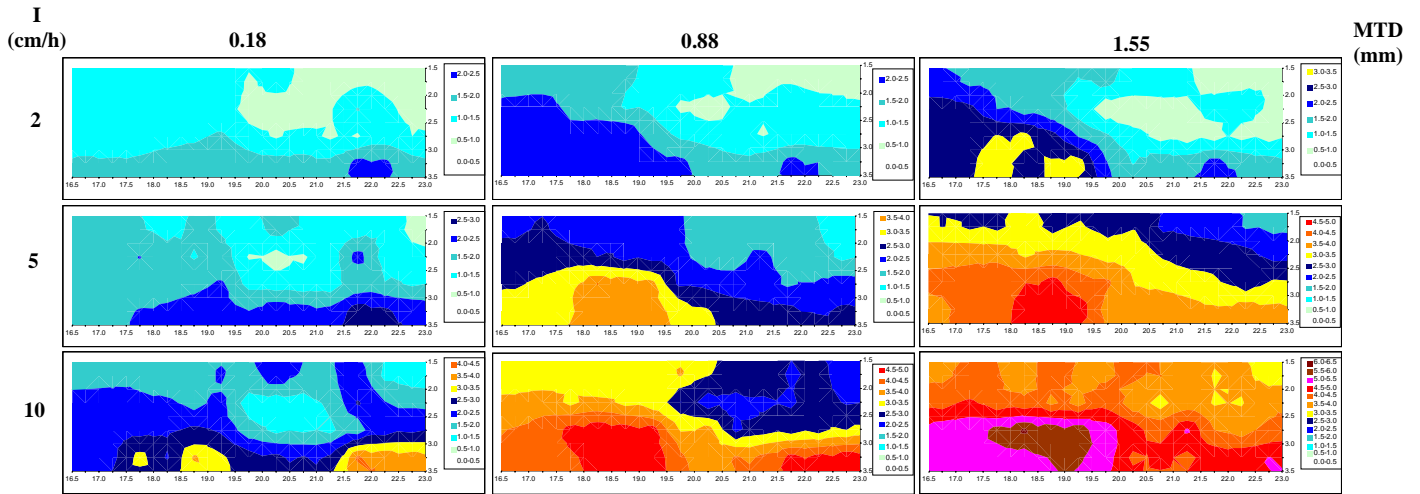


Figure 29 – Results of measurements of WD for the three surfaces and for the three rainfall rates.

### WDs CALCULATION WITH DEFSTRA MODEL

The calculations with the DEFSTRA prediction model were performed considering whether the Ross and Russam or the Gallaway and VERT relationships. The summary of calculations performed is shown in Table 2. The WD calculations were performed with reference both to the theoretic (un-deformed) and to the real geometry of the surface.

Model	Rain intensity	Pavement type	Cod. number
Ross & Russam	2 cm/h	Surface 0	RR 20 018
Ross & Russam	5 cm/h	Surface 0	RR 50 018
Ross & Russam	10 cm/h	Surface 0	RR 100 018
Gallaway et al.	2 cm/h	Surface 0	GA 20 018
Gallaway et al.	5 cm/h	Surface 0	GA 50 018
Gallaway et al.	10 cm/h	Surface 0	GA 100 018
Gallaway et al.	2 cm/h	Surface 1	GA 20 088
Gallaway et al.	5 cm/h	Surface 1	GA 50 088
Gallaway et al.	10 cm/h	Surface 1	GA 100 088
Gallaway et al.	2 cm/h	Surface 2	GA 20 156
Gallaway et al.	5 cm/h	Surface 2	GA 50 156
Gallaway et al.	10 cm/h	Surface 2	GA 100 156
VERT	2 cm/h	Surface 0	VE 20 018
VERT	5 cm/h	Surface 0	VE 50 018
VERT	10 cm/h	Surface 0	VE 100 018
VERT	2 cm/h	Surface 1	VE 20 088
VERT	5 cm/h	Surface 1	VE 50 088
VERT	10 cm/h	Surface 1	VE 100 088
VERT	2 cm/h	Surface 2	VE 20 156
VERT	5 cm/h	Surface 2	VE 50 156
VERT	10 cm/h	Surface 2	VE 100 156

Table 2– Set of WD calculations implemented in DEFSTRA computer program.

An example of the results of DEFSTRA program is shown in the Figure 30, as a chromatic contour curves diagram, for one case among those included in Table 2 (VE 20 088). The Figure 30 refers to the whole of the physical model.

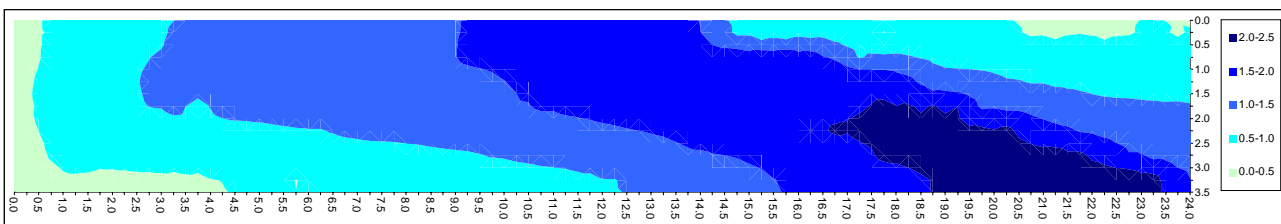


Figure 30 – Example of results in terms of WD (in mm) for the case VE 20 088 for entire model surface.

Figure 31, instead, shows the results of nine cases among those included in Table 2, with reference to the un-deformed surface, in the reference area shown in Figure 28.

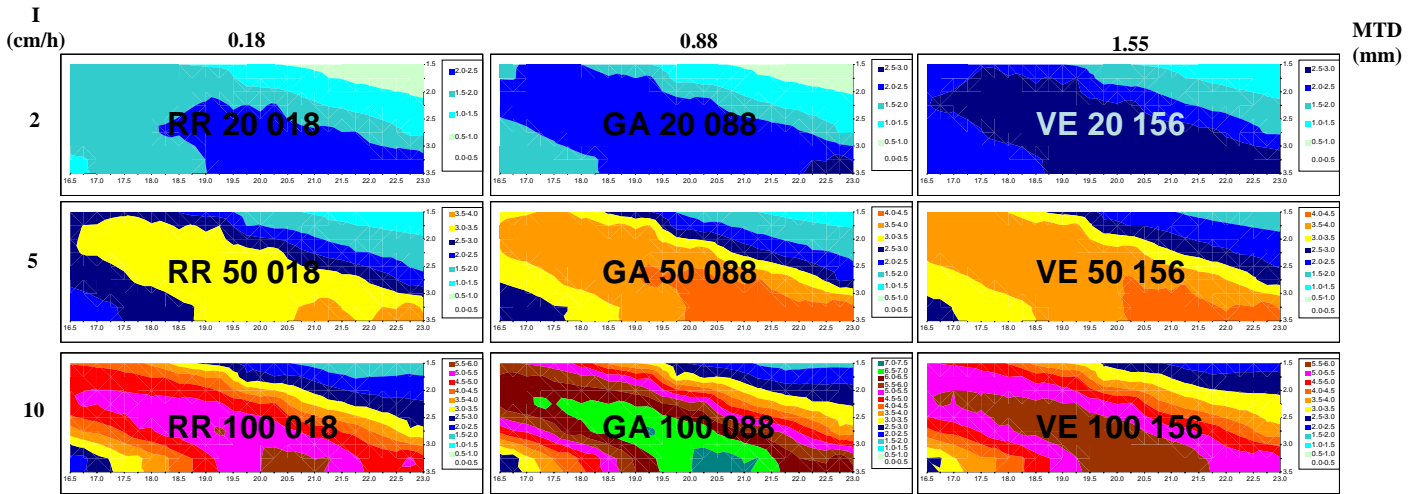


Figure 31 – Examples of results in terms of WD (in mm) for 9 cases for the reference area.

## MODEL VALIDATION: COMPARISON BETWEEN MEASURED AND ESTIMATED WDS

### a) with reference to undeformed theoretical surface

The validation of the DEFSTRA model has been performed comparing, in a first phase, the results of the computer program (WDE: estimated WD) in the reference area for the un-deformed surface with the respective measured WD (WDM). The high number of comparisons to be performed to evaluate the theoretic-experimental formulation estimating WD with the best accordance with WD measured, has been induced the authors to organize the results in the special tables. In such charts, each of the cells of the reference area (where the measurements of WD have been made) has been divided in further 4 parts. In the subcell SO (n. 1) the value of WD is reported (in mm); in the other subcells the symbols (+, - and =) are included to quantify the difference among WDM and WDE calculated according to the 3 formulations (VERT, Gallaway and Ross & Russam). In the tables of Figure 32, simple parameters are also included for appraising the average variations between WDM and WDE (mean of variations  $WDM-WDE$  and absolute mean of variations  $|WDM-WDE|$ ); the means of the WDM and WDE values of all the cells of reference area are also reported. In the Figure 32 such charts related for three meaningful cases are shown.

The differences between the WDE and the WDM can be attributed to one of the following principal causes:

1. geometry variability between theoretic and real surface;
2. geometry variability caused following the building of the surfaces 1 and 2 on top the surface 0;
3. variability inside the generic cell 0.5x0.5 m of the WDE, of the WDM, of the rainfall intensity  $I_j$  and the pavement texture MTD.

On the basis of the aforesaid intrinsic variability do not completely controllable for both the DEFSTRA model and the real scale model, the authors considered the estimated WD conforming to those measured when the absolute variation, in comparison to the measured WD, is less than 25%. Vice versa, if the absolute variations are more then 100%, the disagreement between the estimated WD and measured WD has been considered quite sure.

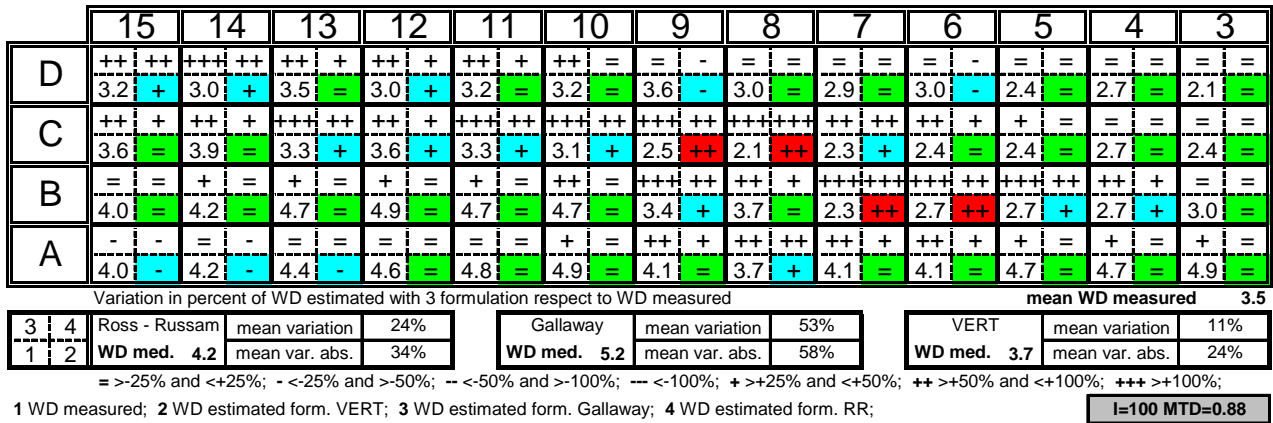
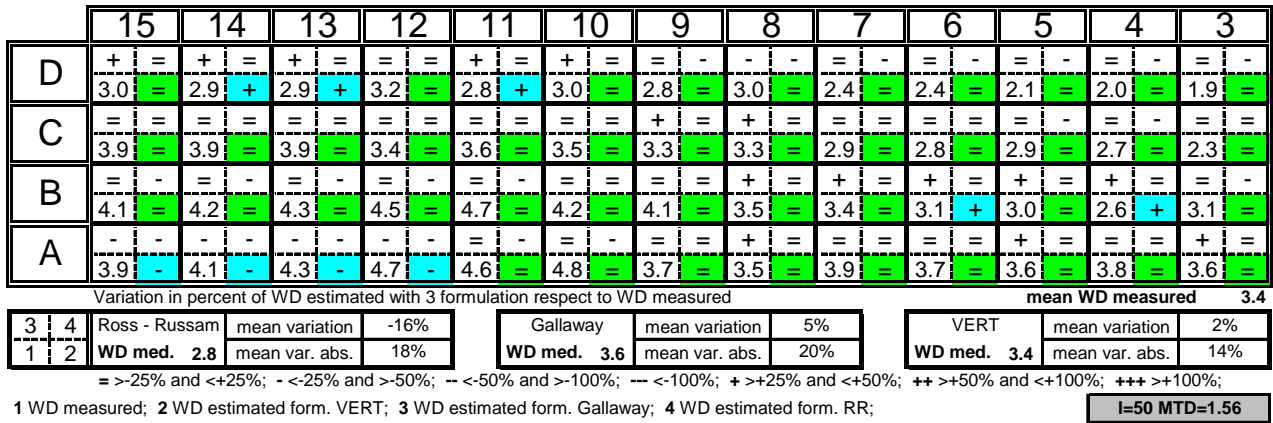
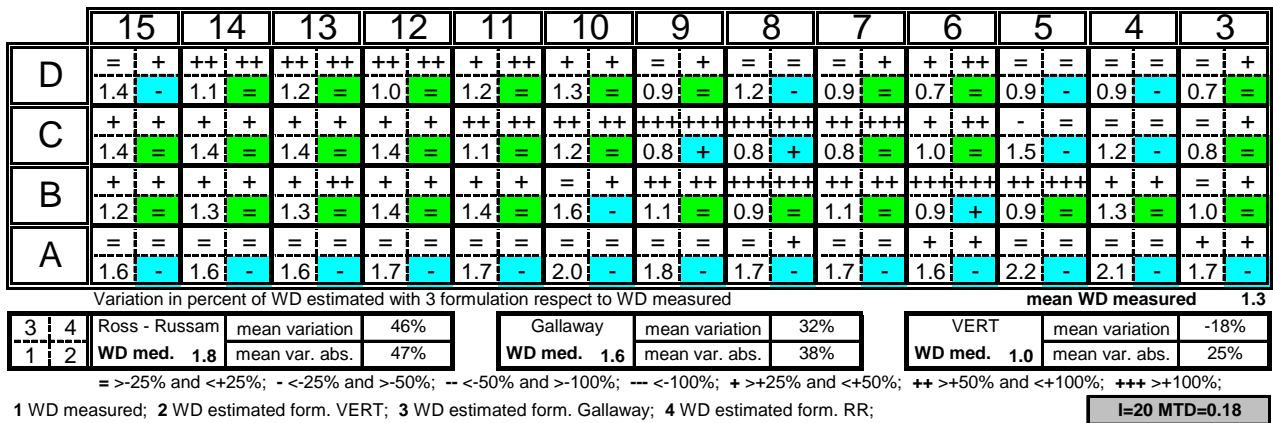


Figure 32 – Chart to compare WDE and WDM.

According to such comparative formulation, the following considerations are possible:

- For the *surface 0*, the WDE estimated with the Ross and Russam formulation and with the Galloway formulation (with MTD=0.18 mm) are comparable among them, but they are notably greater to those measured (40-50% mean variations for I=20, of 70-80% for I=50 and of 110% for I=100); vice versa, for the WDE estimated with the VERT formulation (with MTD=0.18 mm), always less than WD estimated with the other two formulations, the differences with the measured WD are notably less, reaching, in this case, absolute mean variations around 25% for the three rainfall intensities. The calculation of the average of the WDE estimated with the VERT formulation for the 52 cells of the reference area, shows, with respect to measured WD, negative variations around -20% for the middle-low rainfall intensities (20 and 50) and of -9% for the I=100.
- For the *surface 1*, the WDE estimated with the Galloway formulation (with MTD=0.88 mm) are systematically higher than the WDM (128% mean variations for I=20, of 39% for I=50 and of 58% for I=100). As in precedence, for the WDE estimated with the VERT formulation (with MTD=0.88 mm), always less than WDE estimated with the of Galloway formulation, the absolute mean variations in comparison to the WDM measurements are always in the 25% order for the middle-high rainfall

intensities (50 and 100) but they reach 36% for  $I=20$ . The calculation of the average for the WDE estimated with the VERT formulation for the 52 cells of the reference area, shows, with respect to the measured WD, positive variations of 6-8% for the middle-high rainfall intensities (50 and 100) and positive variations of 19% for the  $I=20$ .

- For the *surface 2*, the WDE estimated with the Gallaway formulation (with  $MTD=1.56$  mm) are higher than the WDM (150% mean variations for  $I=20$ , of 20% for  $I=50$  and of 38% for  $I=100$ ). For the middle value of the rain intensity (that is also the more uniform intensity on the surface), the variations result less than 25%, which would induce to show a good correspondence of the formulation of Gallaway for the surfaces with high textured pavements. For the WDE estimated with the VERT formulation (with  $MTD=1.56$  mm), always less than WDE estimated with the Gallaway formulation, the absolute mean variations in comparison to the WDM measurements are always inferior of 25% for the rainfall intensities medium-high (50 and 100) but they reach 74% for  $I=20$ . The calculation of the average of the WDE estimated with the VERT formulation for the 52 cells of the reference area, shows, with respect to the measured WD, positive variations of 7% for high rainfall intensity, zero variation for medium rainfall intensity, and positive variations of 33% for the  $I=20$ .
- The low value of rain intensities generally give WD values on the surface which are quite independent from the geometry and from the pavement texture.

These observations, deduced by the systematic comparison among the measured and estimated WDs on the theoretic surface with the three examined formulations, allow to conclude that the VERT formulation gives likely the best prediction of the distribution of the WD on the road surfaces having a given texture, in the whole range of the considered rainfall intensities. The differences found in this case between the WDM and the WDE can be probably caused, in greater part, by the difference of the theoretic surface in comparison to the real one.

## b) with reference to deformed real surface

In calculating the WDs, the DEFSTRA model cannot take into account a deformed pavement surface as the one measured on the physical full scale model. To still demonstrate the reliability of the DEFSTRA approach, a calculation "by hand" of the WDs was performed, with reference to the biggest "real" flow path lines given by the DEFSTRA model and shown in Figure 33.

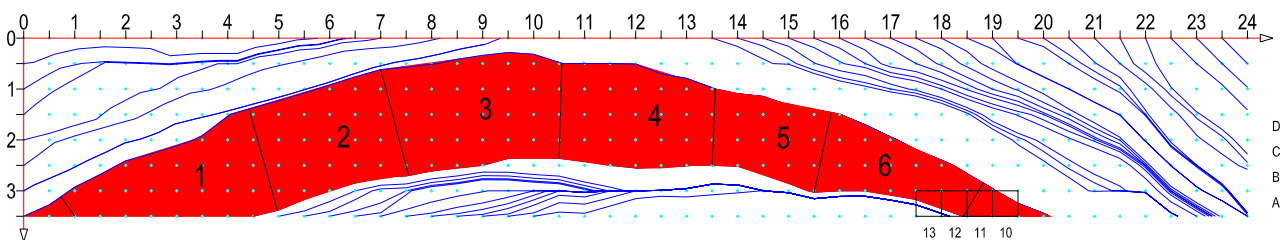


Figure 33 – Biggest flow path line for WD calculus "by hand" with reference to "real" surface 0.

The WD values calculated "by hand" for the three different rain intensities, with reference to the real surface of the model and to the VERT formulation, are shown in Figure 34 together with the measured ones and the calculated ones, the latter with reference to the un-deformed theoretic surface. As it can be clearly seen, the calculated WD values becomes very similar to the measured ones when the real deformed surface is taken into account. This results confirms those given in the previous paragraph, pointing out the higher ability in predicting the WD on a road surface of the DEFSTRA model when fitted with the VERT formulation.

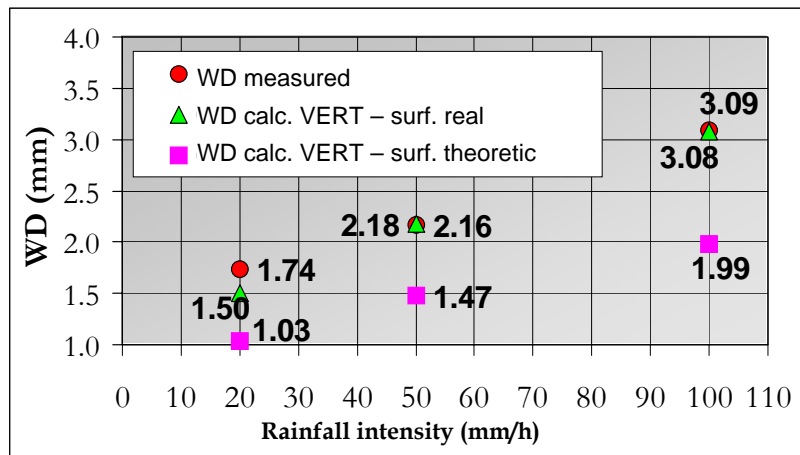


Figure 34 – WD comparing with reference to “real” and to “theoretic” surface 0.

## CONCLUSIONS

To validate the DEFSTRA prediction model calculating the water film depths on a road pavement, an experimental program with a full scale road surface constructed in the road laboratory of the University of Florence was performed.

The full scale model is characterized by a constant longitudinal slope and by varying transversal slopes and is equipped with an artificial rain system able to simulate rainfall of different intensities.

Several measures of water depth have been made on three surfaces with different texture and has been compared with the calculated WD values with the DEFSTRA model fitted with three different formulations of the water depth prediction algorithm.

The computer program DEFSTRA has been also modified to allow to account for rainfall intensities non constant on the surface as the artificial rain system was not able to provide uniform rain intensities over the whole surface of the physical model.

The intense activity of validation has shown that DEFSTRA model, fitted with the VERT formulation, is able to predict, with acceptable reliability (generally less than 25%), the distribution of water depths on a road pavement with known geometric characteristics and surface texture.

The validated DEFSTRA model can be applied to evaluate the water film depth on an existing pavement surface once its geometric and texture characteristics are known. This allow to perform safety analysis characterized by greater reliability since the friction available can be calculated taking care of the real water film thicknesses existing on the pavement.

## REFERENCES

CEN TC 227, prEN 13036-1, 2000. Surface Characteristics - Test Methods – Part 1 : *Measurement of pavement surface macrotexture depth using a volumetric technique.*

C.N.R.-Bollettino ufficiale, 1983 – A. XVII- n.94. *Norme per la Misura delle Caratteristiche Superficiali delle Pavimentazioni. Metodo di Prova per la Misura della Macro-Rugosità Superficiale di Pavimentazioni Stradali ed Aeroportuali.*

Di Volo, N., VERT, 1999. *Vehicle Road Tyre Interaction: Full Integrated and Physical Model for Handling Behaviour Prediction in Potential Dangerous Situation.* Contract n. BRPR-CT97-0461. Task 1. *Influence of Water Thickness on Friction Available. Review of the Water Runoff Models.*

Domenichini, L., Loprencipe, G., 1997. *Analisi dell’Andamento Plano-Altmetrico dei Tracciati in Relazione alle Caratteristiche di Deflusso Idrico.* Convegno SIIV: “La Sicurezza Stradale: strategie e strumenti dell’ingegneria delle infrastrutture viarie” – Pisa, 29-30 ottobre 1997.

Domenichini, L., Remedica, G., 1992. *Condizioni di Deflusso su Piani Stradali in Zone di Transizione.* Atti del XXIII Convegno di Idraulica e Costruzioni Idrauliche, Firenze.

Domenichini, L., Cera, L., 1994. *Distribuzione Areale dei Veli Idrici su Piani Stradali*. Atti del XXII Convegno Nazionale Stradale AIPCR, Perugia.

Guerrini, G.N., 2003. *Studio Sperimentale sulla Variabilità dello Spessore del Velo Idrico su una Pavimentazione Stradale in Funzione delle Caratteristiche Superficiali*. Tesi di laurea in Ingegneria Civile Trasporti, Università degli Studi di Firenze.

Loprencipe, G., 1994. *Modello per la Determinazione della Distribuzione Areale dei Veli Idrici su una Pavimentazione Qualsiasi in Funzione delle Caratteristiche Geometriche e dell'Intensità di Pioggia*. Tesi di laurea in Ingegneria Civile Trasporti, Università degli Studi di Roma "La Sapienza".

Mancosu, F., Parry, A., La Torre, F., 2000. *Friction Variation Due To Speed and Water Depth*. Proc. SURF 2000 4<sup>th</sup> Int. Symposium on Surface Characteristics, Nantes, March 2000.

NCHRP Web Doc 16, 1998. *Improved Surface Drainage of Pavements: Final Report*. <http://www.nap.edu/openbook/nch016>.

Ross, N.F., Russam, K., 1968. *The Depth of Rain on Road Surface*. Road Research Laboratory, Ministry of Transport. RRL Report LR 236.

Università degli Studi di Firenze, VERT, 2000. *Vehicle Road Tyre Interaction: Full Integrated and Physical Model for Handling Behaviour Prediction in Potential Dangerous Situation*. Contract n. BRPR-CT97-0461. Task 1 : *Influence of Water Thickness on Friction Available, sub task 1.1: Flow Models for Computing Water Runoff Depths and Software Development for Modelling Surface Drainage and Predicting Water Thickness*.

## **ACKNOWLEDGEMENTS**

The Authors wish to acknowledge the very helpful and valuable co-operation offered during implementation the experimental activities by the technician of Road Laboratory, Paolo Bencini , the technician of the Land Survey Laboratory, Daniele Ostuni, the engineers Nicola Guerrini, Francesca Pecchioli and Chiara Lorenzini and to the Valli Zabban Company for the test surfaces mix design and material supplying.

A special thank to Michel Gothié, of the CETE Laboratory in Lyons, for providing limnimeter device to measure water depths and to Francesca La Torre for her valuable support during the analysis of the VERT research project results.

A warm gratitude to Prof. Gianrenzo Remedia with whom the initial ideas for the formulation of the water depth prediction model and for the design of the full scale physical model to validate it were discussed.

.